



Research paper

# Kinetic, spectroscopic and *in silico* characterization of the first step of the reaction between glutathione and selenite

Iliia A. Dereven'kov<sup>a,\*</sup>, Luciana Hannibal<sup>b</sup>, Pavel A. Molodtsov<sup>a</sup>, Adrian M.V. Brânzanic<sup>c</sup>, Radu Silaghi-Dumitrescu<sup>c</sup>, Sergei V. Makarov<sup>a</sup>

<sup>a</sup> Ivanovo State University of Chemistry and Technology, Sheremetevskiy str. 7, 153000 Ivanovo, Russia

<sup>b</sup> Laboratory of Clinical Biochemistry and Metabolism, Department of General Pediatrics, Adolescent Medicine and Neonatology, Faculty of Medicine, Medical Center - University of Freiburg, 79106 Freiburg, Germany

<sup>c</sup> Department of Chemistry, "Babes-Bolyai" University, Str. Arany Janos Nr. 11, RO-400028 Cluj-Napoca, Romania

## ARTICLE INFO

## Keywords:

Selenium  
Glutathione  
Selenite  
Mechanisms  
Kinetics

## ABSTRACT

Reduction of dietary selenite ( $\text{SeO}_3\text{H}^-$ ,  $\text{SeO}_3\text{H}_2$ ) is an important process *in vivo*, which predominantly involves glutathione (GSH). Although the reaction between selenite and thiols has been studied extensively, its mechanism and the identification of products remain controversial. Herein, we present kinetic, spectroscopic and *in silico* data on the first step of the reaction between GSH and  $\text{SeO}_3^{2-}$  in aqueous solutions of varying acidity. We found that the reaction reversibly produces glutathione-S-selenite ( $\text{GS-SeO}_2^-$ ) absorbing at 259 nm in the UV spectrum. Assignment of the absorption maximum at 259 nm to  $\text{GS-SeO}_2^-$  was performed using TDDFT and mass spectrometry.  $\text{GS-SeO}_2^-$  undergoes protonation in acidic medium to form the corresponding conjugated acid,  $\text{GS-SeO}_2\text{H}$  ( $\text{pK}_a = 1.9$  at 25 °C), which exhibits reduced absorption intensity at 259 nm. According to the kinetic data, the mechanism of  $\text{GS-SeO}_2^-(\text{H}^+)$  formation includes two pathways: (i) nucleophilic substitution of HO-group in biselenite by the thiolate group of GSH, and (ii) nucleophilic substitution of HO-group in selenous acid by the thiol group of GSH. The complex  $\text{GS-SeO}_2^-(\text{H}^+)$  is unstable in aqueous medium and undergoes hydrolysis to initial reactants, which is accelerated by an increase in alkalinity.

## 1. Introduction

Selenium is an essential ultra-microelement to many animal species. It occurs *in vivo* in the form of selenocysteine (Fig. 1A), selenomethionine (Fig. 1B) and others [1]. Selenocysteine is a proteinogenic amino acid and a key component of glutathione peroxidase, thioredoxin reductase, iodothyronine deiodinase, methionine sulfoxide reductase and other enzymes [2–4].

Inorganic salts, i.e. selenites and selenates, are frequently used as a source of selenium in vitamin-mineral supplements [5]. In the human body, selenite is reduced to hydrogen selenide ( $\text{H}_2\text{Se}$ ), which is converted to selenocysteine via the formation of selenophosphate [6]. Excess selenium is toxic for mammals and it is converted *in vivo* to selenocyanate [7], selenosugars [8] and various methylated compounds [9,10]. The reduction of selenite has been highlighted in several works. For example, selenite can be reduced by super-reduced cobalamin (vitamin  $\text{B}_{12}$ ) [11], thiols [12–14], hydrogen sulfide [15], ascorbic acid [16], dithionite [17],  $\text{Fe}(0)$  [18] and others.

The main *in vivo* route of the reduction of selenite is the process

involving glutathione (GSH; Scheme 1) [6,13,14,19] and references therein]. One of the key intermediates in this process is selenodiglutathione (selenotrisulfide;  $\text{GS-Se-SG}$ ; Scheme 1). Formation of  $\text{GS-Se-SG}$  as well as other trisulfides has been unambiguously proved in several studies [10,12,20,21]. Selenotrisulfides are relatively stable in acidic conditions and are decomposed in neutral and alkaline medium to  $\text{Se}(0)$  and disulfide [21,22]. Nevertheless, data on the structure of the intermediates formed in the course of the first stages of the interaction of selenite and GSH are speculative. One feature of GSH/selenite systems is that selenite possesses catalytic properties in redox reactions involving GSH, e.g. it accelerates formation of reactive oxygen species [19,23], and increases the rate of resazurin reduction [24]. The catalytic behavior of selenite can be due to the reversible formation of highly reactive intermediates whose structure and properties require thorough investigation.

Possible mechanisms for the reactions between selenite and thiols have been highlighted in previous works. The most thorough mechanistic study has been performed by Kice et al. [20]. In this work, the authors suggest a mechanism of reaction of alkylthiols (*n*- and *t*-BuSH)

\* Corresponding author.

E-mail address: [derevenkov@gmail.com](mailto:derevenkov@gmail.com) (I.A. Dereven'kov).

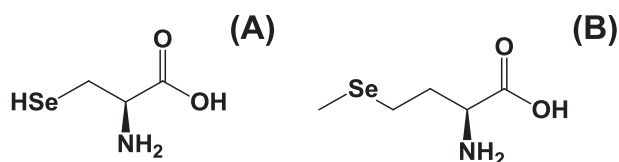
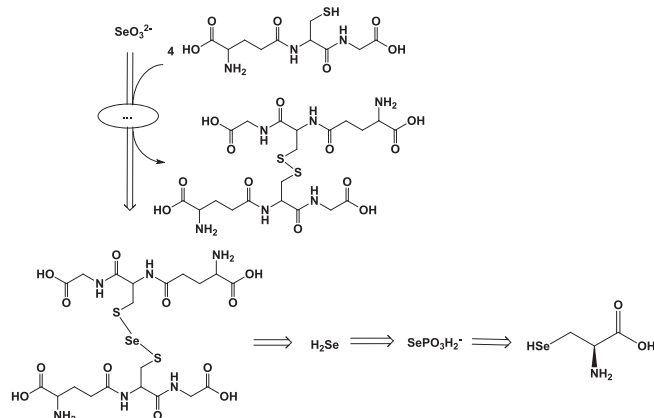
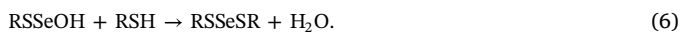


Fig. 1. Structures of selenocysteine (A) and selenomethionine (B).



Scheme 1. In vivo pathway of assimilation of inorganic selenium.

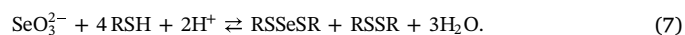
with selenite in water/dioxane mixtures, which involves reversible formation of alkylthioseleninic acid (RSSeO<sub>2</sub>H) in the course of addition of selenium dioxide to thiol (reactions (1),2). RSSeO<sub>2</sub>H is reversibly protonated under acidic conditions to give RSSeO<sub>2</sub>H<sub>2</sub><sup>+</sup> (reaction (3)). RSSeO<sub>2</sub>H (or RSSeO<sub>2</sub>H<sub>2</sub><sup>+</sup>) undergoes reaction with a second thiol molecule to give RSSe(O)SR (reaction (4)), which is further transformed to RSSeSR (reactions (5),6).



A similar mechanism for the reaction between selenite and cysteine has been suggested by Forastiere et al. [25], i.e. RSSeO<sub>2</sub>H is formed in neutral and basic media and is further decomposed via two parallel routes, which may or may not involve a second thiol molecule.

The following disadvantages can be drawn out for these mechanisms. (i) Selenium dioxide formation [20] is unlikely from selenite in weakly acidic, neutral and alkaline media, however, the reaction proceeds at considerable rate (even more rapidly than in strongly acidic conditions) under these conditions. (ii) The work presented in [20,25] did not provide direct, unequivocal proof for the formation of RSSeO<sub>2</sub>H species. (iii) The existence of the product of the first step in protonated form (RSSeO<sub>2</sub>H) in neutral or alkaline media is unlikely: acid-base properties of RSSeO<sub>2</sub>H are expected to be comparable with that of seleninic acids, which are protonated in weakly acidic medium (e.g., pK<sub>a</sub> of selenohypotaourine is 5.4 [26]).

Work by Gennari et al focused on the reversibility of the first step of the reaction between cysteine and selenite [14]. However, authors assigned the formed product as selenotrisulfide. Formation of selenotrisulfide requires reaction of selenite with four thiol molecules (reaction (7)) that cannot be a simple and reversible reaction. Likewise, no direct evidence was provided for the identification of the reaction product.



Cui and coworkers investigated the reaction between GSH and SeO<sub>3</sub><sup>2-</sup> by mass spectrometry [12]. The authors observed signals in the mass-spectrum that were assigned as GS-Se-SG and GSSSe<sup>-</sup>. Formation of these species in their work was explained by reactions 8–10, which apparently comprise a complex mechanism including numerous steps.



The present study was motivated by existing controversies on the mechanisms and the products formed in the reactions between glutathione and selenite. We report kinetic, spectroscopic and *in silico* analysis of the first step of the reaction between GSH and selenite, as well as the characterization of the product of this step, i.e. glutathione-S-selenite.

## 2. Experimental

L-glutathione (Sigma; GSH; ≥ 98%), sodium selenite (Alfa Aesar; ≥ 99.5%), 5,5'-dithiobis-(2-nitrobenzoic acid) (Alfa Aesar; ≥ 99.5%) and hydroxocobalamin hydrochloride (Sigma; ≥ 96%) were used without additional purification. The stable isotopic variant of GSH with a mass difference of +3 was purchased from Sigma and used without further purification (Glutathione-(glycine-<sup>13</sup>C<sub>2</sub>, <sup>15</sup>N) trifluoroacetate salt, ≥ 98 atom % <sup>15</sup>N, ≥ 99 atom % <sup>13</sup>C, ≥ 95% (CP), Sigma 683620).

Buffer solutions (acetate, phosphate and borate; 0.1 M) were used to maintain pH during the measurements. Buffer solutions for mass spectrometry were prepared using CHROMASOLV™ LC-MS water, product Nr. 39253, Honeywell, Germany.

The pH values of solutions were determined using Multitest IPL-103 pH-meter (SEMICO) equipped with ESK-10601/7 electrode (Izmeritel'naya tekhnika) filled by 3.0 M KCl solution. The electrode was preliminarily calibrated using standard buffer solutions (pH 1.65–12.45).

Ultraviolet–visible (UV–vis) spectra were recorded on a cryothermostated (± 0.1 °C) Cary 50 UV–Vis spectrophotometer in quartz cells under aerobic conditions. Preliminary experiments showed that the presence of oxygen does not affect the reaction. Kinetics of the reaction between GSH and selenite was studied on a thermostated (± 0.1 °C) RX2000 (Applied Photophysics, UK) rapid mixing stopped-flow accessory connected to Cary 50 spectrophotometer. Experimental data were analyzed using Origin 7.5 software.

Equilibrium constants were calculated using Eq. (11) [27].

$$A = \frac{A_0 + A_\infty K [\text{SeO}_3^{2-}]}{1 + K [\text{SeO}_3^{2-}]}, \quad (11)$$

[SeO<sub>3</sub><sup>2-</sup>] is the selenite concentration in solution, M; A, A<sub>0</sub>, A<sub>∞</sub> are absorbances at the monitoring wavelength for the complex of selenite with GSH at a particular selenite concentration, for the starting GSH, and for the final complex, respectively; K is equilibrium constant, M<sup>-1</sup>.

Calculation of pK<sub>a</sub> value was performed using Eq. (12).

$$A = A_1 + (A_2 - A_1) \frac{10^{\text{pH}}}{10^{\text{pH}} + 10^{\text{pK}_a}}, \quad (12)$$

A, A<sub>1</sub>, A<sub>2</sub> are absorbances at the monitoring wavelength for the compound at a particular pH, for the protonated species, and for the deprotonated species, respectively.

For DFT calculations, the B3LYP functional and the def2-SV(P) basis set were employed, in geometry optimizations and subsequent time-dependent (TDDFT) (N = 10 states) procedures within the Gaussian software package [28].

ESI mass spectrometry measurements were performed on a Sciex 6500 + triple quadrupole mass spectrometer (Sciex). The instrument

was set up on the low-mass detection mode to monitor  $m/z$  from 100 to 1000 Da. Detection of glutathione and selenite species was performed in the negative mode. The temperature was set at 100 °C, the declustering potential at -60 Volts and the entrance potential at -10 Volts. Each measurement was an average of 10 scans. Direct injection of the reactants upon mixing was performed with minimal delay (30–45 s) using a gas-tight Hamilton syringe hosted at and driven by an automated infusion accessory. All the experiments were performed at room temperature (23–25 °C). Data analysis was performed with built-in software Analyst (Sciex). Experiments were performed either in the presence of 0.1% (w/v) ammonium formate pH 6.8 (neutral conditions) or 0.1% (v/v) formic acid pH 2.1 (acidic conditions) as the solvents. Stock solutions of 100 mM sodium selenite (Sigma S5261-10G) were prepared freshly by dissolving solid sodium selenite in water (CHROMASOLV™ LC-MS water, 39253 Honeywell, Germany). Stock solutions of 50 mM glutathione or its isotope  $^{15}\text{N}$ - $^{13}\text{C}$ -GSH were made freshly by dissolving the appropriate solid reduced glutathione in water (CHROMASOLV™ LC-MS water, 39253 Honeywell, Germany). Both stock solutions of GSH and selenite were kept on ice and brought to room temperature right before their mixing. Reaction mixtures contained equimolar quantities of GSH and selenite (0.5 mM). MS spectra were collected at intervals of 1 min after mixing for the first 5–10 min, and then at 45 min or 90 min (aging of the reaction mix at room temperature).

### 3. Results and discussion

The reaction of GSH with selenite at pH 7.2 generates a first-step product with absorbance maximum at 259 nm in UV spectrum (Fig. 2). This observation has been reported in earlier works [12–14,20,25]. The same peak is observed in acidic and alkaline media with the exception of strongly acidic and strongly alkaline conditions, where formation of this product is negligible. However, we found that the maximum intensity of the peak at 259 nm depends strongly on selenite concentration and reaches maximum intensity with excess selenite over GSH (Fig. 3). This fact is typical to equilibrium processes, i.e. GSH and selenite are capable of reversibly binding within the first step of the process.

To support regeneration of GSH from its complex with selenite, we mixed GSH with a significant excess of selenite in order to transform GSH to its bound state and then added Ellman's reagent (5,5'-dithiobis-(2-nitrobenzoic acid)) or aquacobalamin. Reaction of thiols with Ellman's reagent results in formation of the product with absorption peak at 412 nm, whereas aquacobalamin tightly binds GSH to give glutathionylcobalamin [29], a complex with characteristic UV-vis

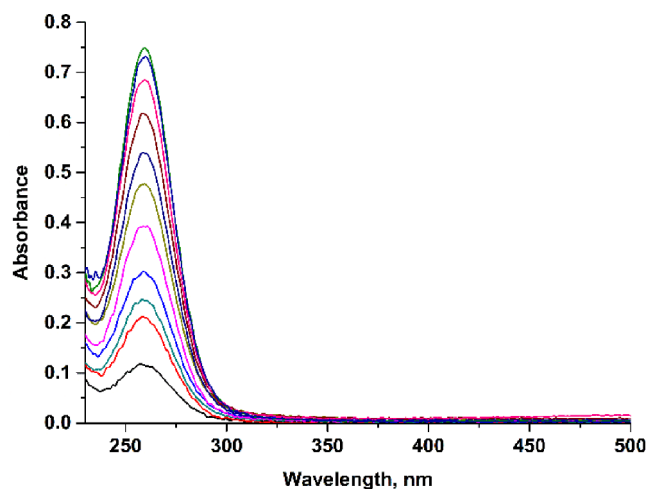


Fig. 2. Maximum of absorption in the UV-vis spectra of GSH/ $\text{SeO}_3^{2-}$  mixtures collected at pH 7.2; 25.0 °C.  $[\text{GSH}]_0 = 1.2 \cdot 10^{-4}$  M;  $[\text{SeO}_3^{2-}]_0 = 5.0 \cdot 10^{-5}$  M (lower spectrum) ...  $8.0 \cdot 10^{-3}$  M (upper spectrum).

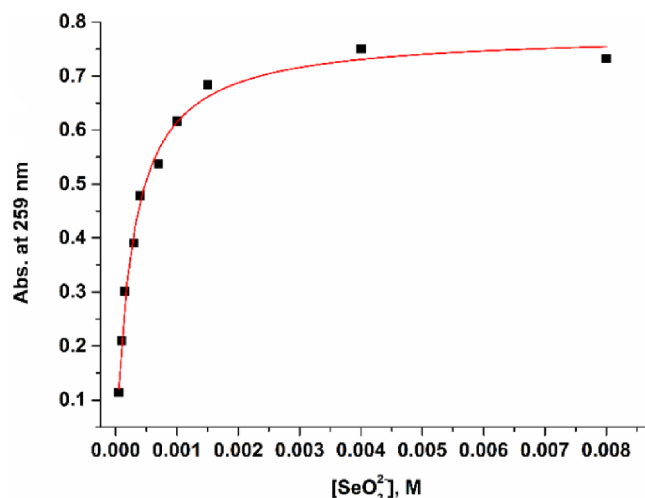


Fig. 3. Plot of maximum absorbance at 259 nm vs.  $[\text{SeO}_3^{2-}]$ .  $[\text{GSH}]_0 = 1.2 \cdot 10^{-4}$  mM; pH 7.2; 25.0 °C.

spectrum [30]. We found that UV-vis spectral changes in the course of the reaction of the GSH/selenite complex with Ellman's reagent (Fig. S1) or aquacobalamin (Fig. S2) are identical to those for the processes involving free GSH, although the latter reactions proceed more rapidly.

Using eq. (11), we determined equilibrium constants for complex formation between GSH and selenite in solutions of varying acidity. The maximum equilibrium constant (ca.  $4000 \text{ M}^{-1}$  at 25 °C) is observed at pH 1...3 and 6.5...7.2 (Fig. 4).

Next, we studied the kinetics of the reaction between GSH and an excess of selenite. Kinetics of a reversible pseudo-first-order reaction can be confused with two schemes, i.e. with (i) a consecutive pathway ( $A \rightarrow B$ ;  $B + A \rightarrow P$ ) and (ii) parallel reactions ( $C \rightarrow P_1$ ;  $C + D \rightarrow P_2$ ) including the decomposition of reactant taken in excess ( $C \rightarrow P_1$ ) [31,32]. Using Ellman's reagent and aquacobalamin, we clearly showed that the product of the studied reaction regenerates GSH that allows to analyze the interaction between GSH and excess selenite as the reversible pseudo-first-order reaction.

Kinetic curves are best described by an exponential equation (Fig. 5) that indicates first order with respect to GSH. The plot of observed rate constants versus  $[\text{SeO}_3^{2-}]$  is provided in Fig. 6. The linear dependence indicates first order with respect to selenite. The value of intercept is indistinguishable from zero at near neutral media and becomes more

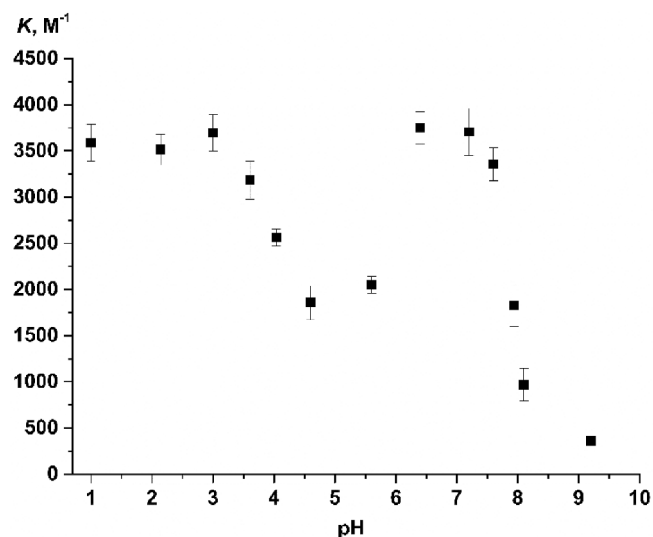


Fig. 4. Dependence of equilibrium constant ( $K$ ) for the reaction between GSH and selenite on pH at 25.0 °C.

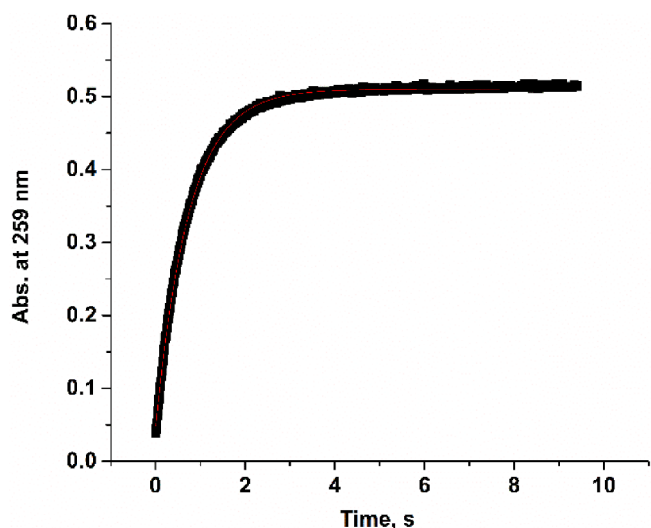


Fig. 5. Typical kinetic curve of the reaction between GSH (0.1 mM) and  $\text{SeO}_3^{2-}$  (1.0 mM) at pH 7.5; 25.0 °C.

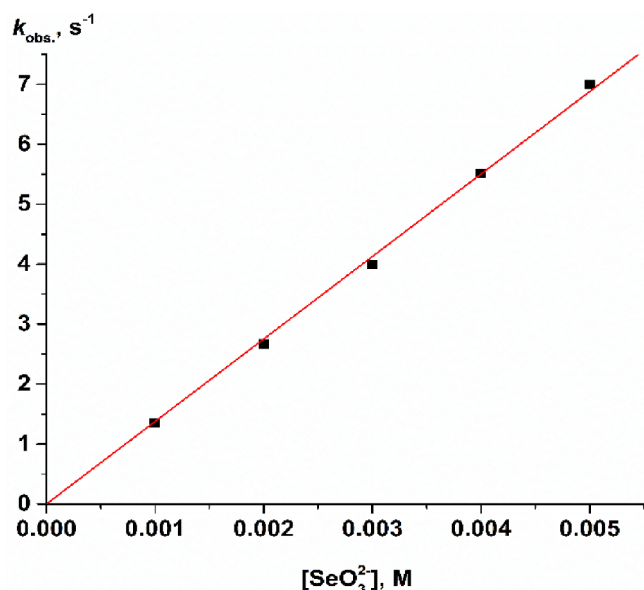


Fig. 6. Plot of observed rate constants ( $k_{\text{obs}}$ ) vs.  $[\text{SeO}_3^{2-}]$ .  $[\text{GSH}]_0 = 0.1$  mM; pH 7.5; 25.0 °C.

pronounced in acidic (Fig. S3) and alkaline (Fig. S4) conditions. The intercept can be explained by the presence of reverse reaction, i.e. decomposition of the complex between GSH and selenite. The value of the intercept increased upon alkalization (Fig. S5), which is explained by hydrolysis of the complex.

The dependence of reaction rate on pH in weakly acidic, neutral and weakly alkaline conditions is bell-shaped (Fig. 7), suggesting an influence of acid-base properties of both reactants on kinetics. Apparently, one of acid-base equilibria affecting the kinetics is deprotonation of thiol group of GSH (13;  $\text{pK}_a = 8.9$  at 25.0 °C [33]). The second process involves protonation of selenite to biselenite (14;  $\text{pK}_a$  ranges from 6.6 to 8.5 depending on conditions at 25.0 °C [34]). Thus, the reactive species in weakly acidic, neutral and weakly alkaline media are thiolate form of GSH and monoprotonated form of selenite. The plot of rate constant versus pH indicates slight increase upon acidification at pH 1...3, which can be due to the protonation of biselenite to selenous acid (15;  $\text{pK}_a = 2.7$  at 25.0 °C [34]) and the reaction between selenous acid and GSH with protonated thiol group, Fig. 8.

Dependencies of rate constant of forward ( $k'$ ; Fig. 7) and reverse

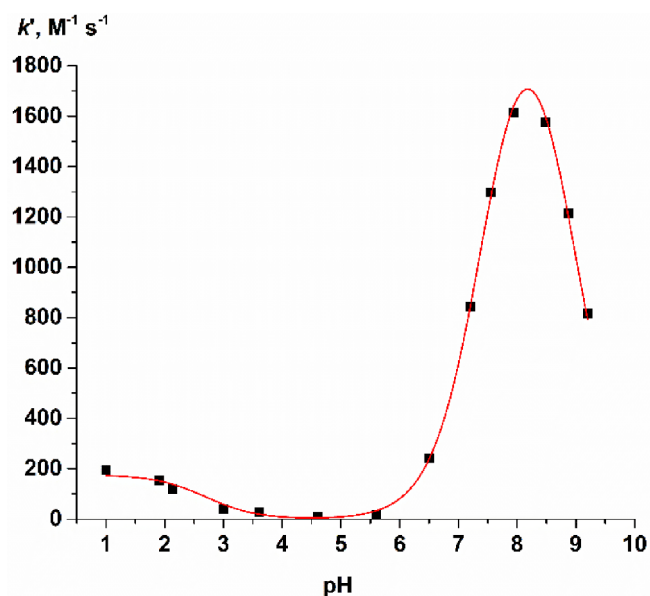
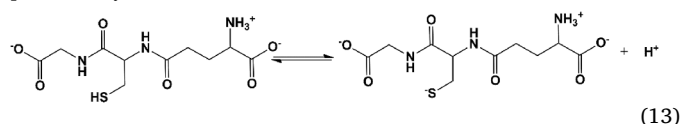


Fig. 7. Dependence of the rate constants of the forward reaction of GSH with selenite ( $k'$ ; slopes of concentration dependencies) on pH at 25.0 °C.

( $k_{\text{int}}$ ; Fig. S5) reactions on pH explains profile of plot of equilibrium constant ( $K = k'/k_{\text{int}}$ ) versus pH (Fig. 4). Plot of  $K$  versus pH exhibits minimum at pH 3.0...6.5 that coincides with minimum of plot of  $k'$  versus pH in this range. Decrease of  $K$  at pH > 7.5 is predominantly provided by an increase of  $k_{\text{int}}$  in this medium.



Taking into account these equilibria, Eq. (16) was expressed.

$$k' = k_1 \frac{10^{\text{pK}_a(\text{SeO}_3\text{H}_2) + \text{pK}_a(\text{GSH})}}{(10^{\text{pH}} + 10^{\text{pK}_a(\text{SeO}_3\text{H}_2)})(10^{\text{pH}} + 10^{\text{pK}_a(\text{GSH})})} + k_2 \frac{10^{\text{pH} + \text{pK}_a(\text{SeO}_3\text{H}^-)}}{(10^{\text{pH}} + 10^{\text{pK}_a(\text{SeO}_3\text{H}^-)})(10^{\text{pH}} + 10^{\text{pK}_a(\text{GSH})})} \quad (16)$$

where  $\text{pK}_a(\text{SeO}_3\text{H}^-)$ ,  $\text{pK}_a(\text{SeO}_3\text{H}_2)$  and  $\text{pK}_a(\text{GSH})$  are acid dissociation constants for  $\text{SeO}_3\text{H}^-$ ,  $\text{SeO}_3\text{H}_2$  and the thiol group in GSH, respectively;  $k_1$  is rate constant for the reaction between GSH with protonated thiol group and  $\text{SeO}_3\text{H}_2$ ;  $k_2$  is rate constant for the reaction between  $\text{GS}^-$  (thiolate form of GSH) and  $\text{SeO}_3\text{H}^-$ . Using  $\text{pK}_a(\text{GSH}) = 8.9$  and  $\text{pK}_a(\text{SeO}_3\text{H}_2) = 2.7$  ( $\text{pK}_a(\text{SeO}_3\text{H}^-) = 7.5$  was determined during fitting),  $k_1 = (1.8 \pm 0.1) \cdot 10^2$  and  $k_2 = (6.7 \pm 0.2) \cdot 10^4 \text{ M}^{-1} \text{ s}^{-1}$  were obtained.

Finally, we assessed the rate of the subsequent step of the reaction between GSH and selenite accompanied by a reduction of absorbance intensity at 259 nm. As can be seen from Fig. S6, this step proceeds much slower than the first step and the primary product of the reaction between GSH and selenite is more stable in the presence of higher selenite concentrations.

To identify the product, we performed MS measurements under acidic (pH 2.1) and neutral conditions (pH 6.8). Formation of a species with  $m/z$  at 418 was observed upon mixing GSH with an equimolar amount of selenite both under acidic and neutral conditions (Figs. 8 and S7). Use of isotopically labeled glutathione with a mass difference of 3+ ( $^{15}\text{N}$ - $^{13}\text{C}_2$ -GSH) permitted the identification of a species at  $m/z$  421. These  $m/z$  can be attributed to  $\text{GSSeO}_2^-$  adduct formed upon conjugation of selenite with GSH. Evidence for the formation of the product

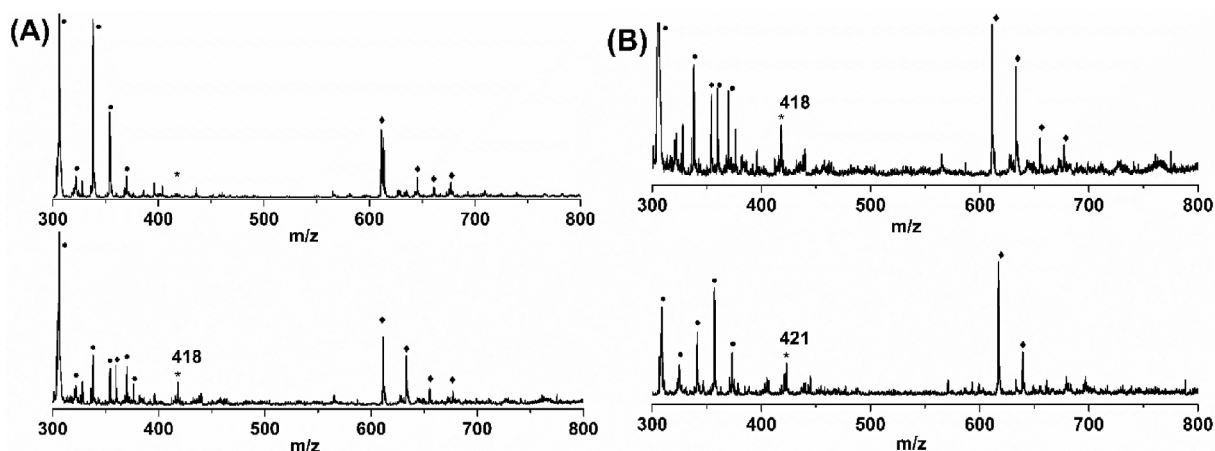


Fig. 8. Mass-spectra of GSH (upper spectrum, panel A), GSH/selenite mixture (bottom spectrum, panel A, and upper spectrum, panel B) and  $^{15}\text{N}$ - $^{13}\text{C}_2$ -GSH/selenite mixture (bottom spectrum, panel B) recorded after mixing of reactants at pH 6.8. Signals of GSH and GSSG ions or their Na-derived versions and  $\text{NH}_3$ -adducts are indicated by  $\bullet$  and  $\blacklozenge$ , respectively.

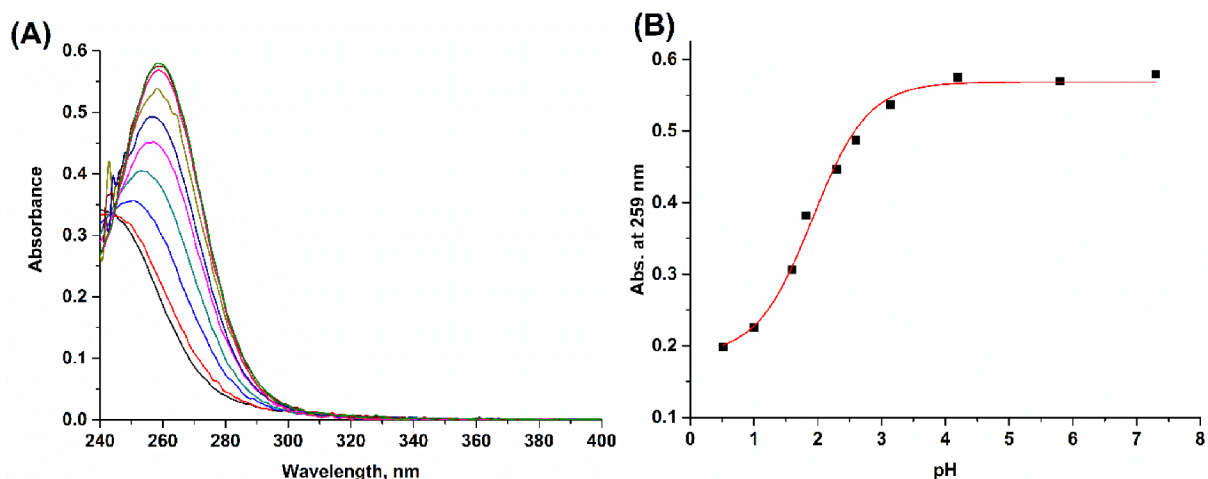


Fig. 9. UV spectra of  $\text{GS-SeO}_2^-(\text{H}^+)$  collected at pH 0.5 to 7.2 (A) and the plot of absorbance at 259 nm versus pH (B).  $\text{GS-SeO}_2^-(\text{H}^+)$  was prepared by mixing GSH ( $1 \cdot 10^{-4}$  M) with selenite ( $2 \cdot 10^{-2}$  M) at  $25.0^\circ\text{C}$ .

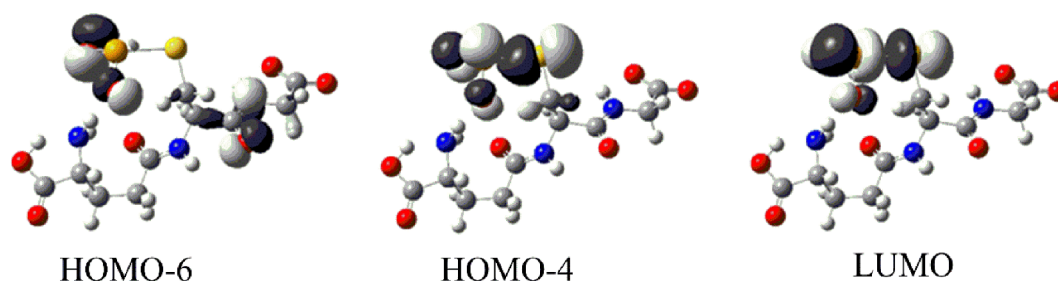


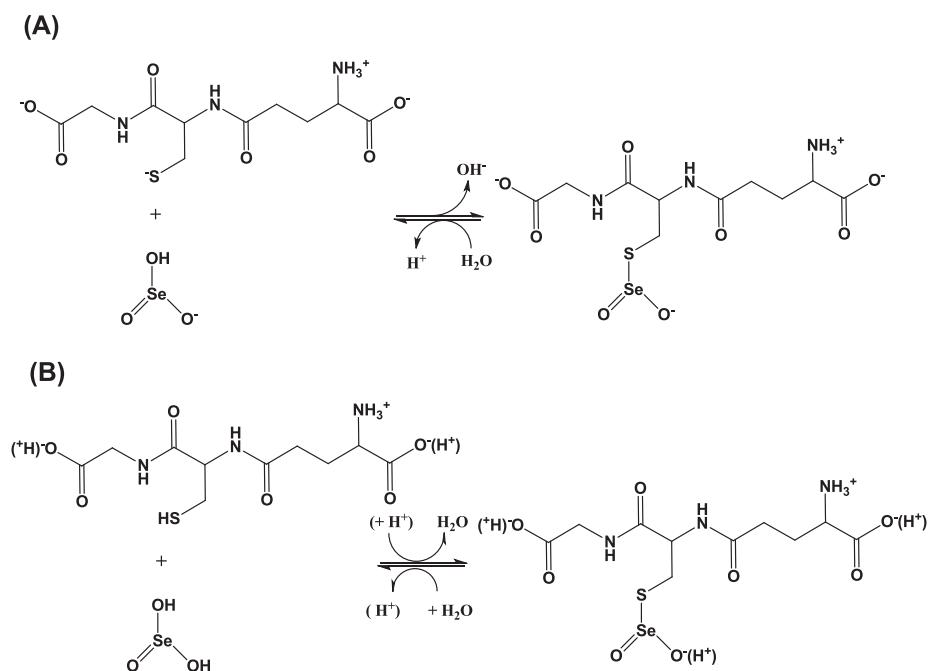
Fig. 10. Main orbitals that contribute to the DFT-computed UV-vis spectrum of  $\text{GS-SeO}_2^-$ .

with  $m/z = 418$  was presented in an earlier ESI-MS study [12], but this peak was attributed to  $\text{GSSe}^-$ . However, since species with  $m/z = 418$  is formed very rapidly, after the mixing of glutathione and selenite, we assume that it cannot be  $\text{GSSe}^-$ .

Further examination of the equilibrium between protonated and deprotonated species of  $\text{GS-SeO}_2^-(\text{H}^+)$  was conducted by recording UV spectra at pH 0.5 to 8.0. The intensity of the peak at 259 nm is substantially decreased at  $\text{pH} < 3$  (Fig. 9A; extinction coefficients for deprotonated and protonated species are  $5700$  and  $1900 \text{ M}^{-1} \text{ cm}^{-1}$  at 259 nm), which can be due to the protonation of  $\text{SeO}_2^-$  group of  $\text{GS-SeO}_2^-$ . It is unlikely that protonation of groups distant from the S-Se motif (i.e., carboxylates) can be reflected in the UV spectrum.  $\text{pK}_a(\text{GS-}$

$\text{SeO}_2\text{H}) = (1.9 \pm 0.1)$  ( $25.0^\circ\text{C}$ ) was determined by fitting plot of absorbance versus pH (Fig. 9B) to eq. (12).

The assignment of the experimentally-observed UV peak to  $\text{GS-SeO}_2^-$  was further verified using time-dependent DFT (TDDFT) calculations. The strongest contribution to the DFT-derived UV-vis spectrum of  $\text{GS-SeO}_2^-$  is at 296 nm (computed extinction coefficient:  $3235 \text{ M}^{-1} \text{ cm}^{-1}$ ), arising primarily from a HOMO-4  $\rightarrow$  LUMO excitation. The second strongest contribution, closely overlapping at 278 nm (computed extinction coefficient:  $1325 \text{ M}^{-1} \text{ cm}^{-1}$ ) arises primarily from a HOMO-6  $\rightarrow$  LUMO excitation. Other contributions are significantly lower in intensity. These computed wavelengths are in reasonable agreement with experiment, considering the accuracy of the



**Scheme 2.** Mechanism of the first step of the reaction between selenite and glutathione in weakly acidic, neutral, weakly alkaline (A) and strongly acidic (B) media.

DFT method [35]. As seen in Fig. 10, the calculated electronic transitions amount to a  $\sigma \rightarrow \sigma^*$  and  $n \rightarrow \sigma^*$  character of the main band expected in the UV-vis spectrum of  $\text{GS-SeO}_2^-$ . On the other hand, the DFT-derived UV-vis spectrum of the protonated version ( $\text{GS-SeO}_2\text{H}$ ) is found to be one order of magnitude weaker and redshifted by 100–150 nm and is therefore not further discussed.

The mechanism of the reaction is shown in Scheme 2. Taking into account the type of reactive species elucidated upon fitting of the plot of rate constant versus pH (Fig. 7), two routes depending on pH can be suggested. In weakly acidic, neutral and weakly alkaline conditions, the reaction proceeds between the thiolate form of GSH and the monoprotonated form of selenite. Deprotonation of the thiol group enhances its nucleophilicity and enables substitution of HO-group in biselenite. Deprotonated selenite species ( $\text{SeO}_3^{2-}$ ) is unlikely to be involved in reaction with GSH or its deprotonated version due to their large negative charge hampering the contact with nucleophiles. In more acidic conditions the reacting species are selenous acid and the thiol form of GSH. Second protonation of selenite increases its electrophilicity and facilitates its interaction with the protonated thiol group. The products of the interaction are glutathione-S-selenite ( $\text{GS-SeO}_2^-$ ) and its conjugated acid ( $\text{GS-SeO}_2\text{H}$ ). S-Se bond in  $\text{GS-SeO}_2^-(\text{H}^+)$  is capable of reacting with water or hydroxide that result in formation of initial reactants.

#### 4. Conclusion

This study provides direct proof that the reaction of selenite with glutathione reversibly produces glutathione-S-selenite ( $\text{GSSeO}_2^-$ ) or its conjugated acidic form ( $\text{GSSeO}_2\text{H}$ ). The reaction involves nucleophilic substitution of the HO-group of biselenite by the thiolate glutathione species or substitution of the HO-group in selenous acid by the thiol form of GSH. The product of the interaction is unstable in aqueous solutions and undergoes decomposition to selenite and GSH and can be stabilized by adding an excess of selenite. The complex glutathione-S-selenite ( $\text{GSSeO}_2^-$ ) undergoes reduction in the presence of an excess of glutathione. The stability of  $\text{GSSeO}_2^-$  in the presence of excess selenite is sufficient to perform a characterization of its reactivity to gain further insights in the complex mechanism of reaction between GSH and selenite.

#### Declaration of Competing Interest

The authors declare that they have no known competing financial interests or personal relationships that could have appeared to influence the work reported in this paper.

#### Acknowledgements

This work was supported by grant of Council on grants of the President of the Russian Federation for state support of young Russian researchers (project MK-1083.2019.3).

#### Appendix A. Supplementary data

Supplementary data to this article can be found online at <https://doi.org/10.1016/j.ica.2019.119215>.

#### References

- [1] H.J. Reich, R.J. Hondal, ACS Chem Biol. 11 (2016) 821–841, <https://doi.org/10.1021/acscchembio.6b00031>.
- [2] V.M. Labunsky, D.L. Hatfield, V.N. Gladyshev, Physiol. Rev. 94 (2014) 739–777, <https://doi.org/10.1152/physrev.00039.2013>.
- [3] R. Brigelius-Flohé, Antioxid. Redox Sign. 33 (2015) 757–760, <https://doi.org/10.1089/ars.2015.6469>.
- [4] M. Iwaoka, K. Arai, Curr. Chem. Biol. 7 (2013) 2–24, <https://doi.org/10.2174/2212796811307010002>.
- [5] J. Zhou, G. Xu, Z. Bai, K. Li, J. Yan, F. Li, S. Ma, H. Xu, K. Huang, Toxicol. Appl. Pharmacol. 289 (2015) 409–418, <https://doi.org/10.1016/j.taap.2015.10.019>.
- [6] K.A. Cupp-Sutton, M.T. Ashby, Antioxidants 5 (2016), <https://doi.org/10.3390/antiox5040042>.
- [7] Y. Anan, M. Kimura, M. Hayashi, R. Koike, Y. Ogra, Chem. Res. Toxicol. 28 (2015) 1803–1814, <https://doi.org/10.1021/acs.chemrestox.5b00254>.
- [8] Y. Kobayashi, Y. Ogra, K. Ishiwata, H. Takayama, N. Aimi, K.T. Suzuki, PNAS 99 (2002) 15932–15936, <https://doi.org/10.1073/pnas.252610699>.
- [9] M. Itoh, K.T. Suzuki, Arch. Toxicol. 71 (1997) 461–466, <https://doi.org/10.1007/s002040050412>.
- [10] H.E. Ganther, Int. J. Toxicol. 5 (1986) 1–5, <https://doi.org/10.3109/10915818609140731>.
- [11] I.A. Derevenkov, D.S. Salnikov, S.V. Makarov, Russ. J. Phys. Chem. A 91 (2017) 2404–2408, <https://doi.org/10.1134/S003602441711005X>.
- [12] S.-Y. Cui, H. Jin, S.-J. Kim, A.P. Kumar, Y.-I. Lee, J. Biochem. 143 (2008) 685–693, <https://doi.org/10.1093/jb/mvn023>.
- [13] J. Kessi, K.W. Hanselmann, J. Biol. Chem. 279 (2004) 50662–50669, <https://doi.org/10.1074/jbc.M405887200>.

- [14] F. Gennari, V.K. Sharma, M. Pettine, L. Campanella, F.J. Millero, *Geochim. Cosmochim. Acta* 124 (2014) 98–108, <https://doi.org/10.1016/j.gca.2013.09.019>.
- [15] M. Pettine, F. Gennari, L. Campanella, B. Casentini, D. Marani, *Geochim. Cosmochim. Acta* 83 (2012) 37–47, <https://doi.org/10.1016/j.gca.2011.12.024>.
- [16] M. Pettine, F. Gennari, L. Campanella, *Chemosphere* 90 (2013) 245–250, <https://doi.org/10.1016/j.chemosphere.2012.06.061>.
- [17] N. Geoffroy, G.P. Demopoulos, *Ind. Eng. Chem. Res.* 48 (2009) 10240–10246, <https://doi.org/10.1021/ie9008502>.
- [18] L. Liang, X. Jiang, W. Yang, Y. Huang, X. Guan, L. Li, *Desalin. Water Treat.* 53 (2015) 2540–2548, <https://doi.org/10.1080/19443994.2013.862868>.
- [19] C.C. Tsen, A.L. Tappel, *J. Biol. Chem.* 233 (1958) 1230–1232.
- [20] J.L. Kice, T.W.S. Lee, S. Pan, *J. Am. Chem. Soc.* 102 (1980) 4448–4455, <https://doi.org/10.1021/ja00533a025>.
- [21] D. Burris, W. Zou, D. Cremer, J. Walrod, D. Atwood, *Inorg. Chem.* 53 (2014) 4010–4021, <https://doi.org/10.1021/ic402909t>.
- [22] J. Zhang, H. Lu, X. Wang, *Biol. Trace Elem. Res.* 125 (2008) 13–21, <https://doi.org/10.1007/s12011-007-8044-0>.
- [23] S. Misra, M. Boylan, A. Selvam, J.E. Spallholz, M. Björnstedt, *Nutrients* 7 (2015) 3536–3556, <https://doi.org/10.3390/nu7053536>.
- [24] W.A. Prütz, *J. Chem. Soc., Chem. Commun.* 1639–1640 (1994), <https://doi.org/10.1039/C39940001639>.
- [25] D.O. Forastiere, E.B. Borghi, P.J. Morando, *Helv. Chim. Acta* 90 (2007) 1152–1159, <https://doi.org/10.1002/hlca.200790114>.
- [26] K.L. House, R.B. Dunlap, J.D. Odom, Z.-P. Wu, D. Hilver, *J. Am. Chem. Soc.* 114 (1992) 8573–8579, <https://doi.org/10.1021/ja00048a033>.
- [27] I.A. Dereven'kov, D.S. Salnikov, S.V. Makarov, M. Surducun, R. Silaghi-Dumitrescu, G.R. Boss, *J. Inorg. Biochem.* 125 (2013) 32–39, <https://doi.org/10.1016/j.jinorgbio.2013.04.011>.
- [28] Gaussian 09, Revision E.01, M.J. Frisch, G.W. Trucks, H.B. Schlegel, G.E. Scuseria, M.A. Robb, J.R. Cheeseman, G. Scalmani, V. Barone, B. Mennucci, G.A. Petersson, H. Nakatsuji, M. Caricato, X. Li, H.P. Hratchian, A.F. Izmaylov, J. Bloino, G. Zheng, J.L. Sonnenberg, M. Hada, M. Ehara, K. Toyota, R. Fukuda, J. Hasegawa, M. Ishida, T. Nakajima, Y. Honda, O. Kitao, H. Nakai, T. Vreven, J.A. Montgomery, Jr, J.E. Peralta, F. Ogliaro, M. Bearpark, J.J. Heyd, E. Brothers, K.N. Kudin, V.N. Staroverov, R. Kobayashi, J. Normand, K. Raghavachari, A. Rendell, J.C. Burant, S. S. Iyengar, J. Tomasi, M. Cossi, N. Rega, J.M. Millam, M. Klene, J.E. Knox, J.B. Cross, V. Bakken, C. Adamo, J. Jaramillo, R. Gomperts, R.E. Stratmann, O. Yazyev, A.J. Austin, R. Cammi, C. Pomelli, J.W. Ochterski, R.L. Martin, K. Morokuma, V.G. Zakrzewski, G.A. Voth, P. Salvador, J.J. Dannenberg, S. Dapprich, A.D. Daniels, Ö. Farkas, J.B. Foresman, J.V. Ortiz, J. Cioslowski, D.J. Fox, Gaussian, Inc., Wallingford CT, 2009.
- [29] G.L. Ellman, *Arch. Biochem. Biophys.* 82 (1959) 70–77, [https://doi.org/10.1016/0003-9861\(59\)90090-6](https://doi.org/10.1016/0003-9861(59)90090-6).
- [30] L. Xia, A.G. Cregan, L.A. Berben, N.E. Brasch, *Inorg. Chem.* 43 (2004) 6848–6857, <https://doi.org/10.1021/ic040022c>.
- [31] Á. Balogh, G. Lente, J. Kalmár, I. Fábíán, *Int. J. Chem. Kin.* 47 (2015) 773–782, <https://doi.org/10.1002/kin.20960>.
- [32] J. Kalmár, G. Lente, I. Fábíán, *Inorg. Chem.* 52 (2013) 2150–2156, <https://doi.org/10.1021/ic302544y>.
- [33] D.L. Rabenstein, *J. Am. Chem. Soc.* 95 (1973) 2797–2803, <https://doi.org/10.1021/ja00790a009>.
- [34] F. Séby, M. Potin-Gautier, E. Giffaut, G. Borge, O.F.X. Donard, *Chem. Geol.* 171 (2001) 173–194, [https://doi.org/10.1016/S0009-2541\(00\)00246-1](https://doi.org/10.1016/S0009-2541(00)00246-1).
- [35] A.A.A. Attia, D. Cioloboc, A. Lupan, R. Silaghi-Dumitrescu, *J. Inorg. Biochem.* 165 (2016) 49–53, <https://doi.org/10.1016/j.jinorgbio.2016.09.017>.